DOI: 10.1002/ejic.200901148

Acridone-Benzimidazole Ring-Fused Ligands: A New Class of Sensitizers of Lanthanide Luminescence via Low-Energy Excitation

Emmanuel Deiters,[a] Frédéric Gumy,[a] and Jean-Claude G. Bünzli*[a,b]

Keywords: Tridentate ligands / Luminescence / Energy transfer / Lanthanides / Sensitizers / Radiative lifetime / Sensitization efficiency

Two monotopic tridentate ligands, namely H**L**$^{\mathbf{AB1}}$ and H**L**$^{\mathbf{AB2}}$ have been synthesized which feature an acridone chromophore fused on a benzimidazolepyridine framework. They differ from each other by their connection points between a *N*-methylacridone and a *N*-methylbenzimidazole chromophoric moieties. Both ligands self-assemble with Ln^{III} ions in neat acetonitrile to form thermodynamically stable neutral complexes of general formula [Ln(**L**$^{\mathbf{ABX}}$)$_3$] ($\log\beta_{13}$ in the range 22–25). Subsequent photophysical investigations conducted in the same solvent demonstrate that ligand H**L**$^{\mathbf{AB1}}$ sensitizes europium luminescence (Q^{L}_{Eu} = 10 % and τ_{Eu} = 0.93 ms) whereas ligand H**L**$^{\mathbf{AB2}}$ sensitizes the luminescence of NIR-emitting Ln^{III} ions, in particular Yb^{III} (Q^{L}_{Yb} = 0.86 % and τ_{Yb} = 29.3 μs). The sensitization efficiencies η_{sens} of both ligands have been determined for these two complexes and found to be around 50–60 %. The main advantage of these ligands is their excitation wavelength which lies in the visible range (410–430 nm).

Introduction

Lanthanide complexes are the subject of intensive research efforts in view of their unique optical properties including easy recognizable emission lines, large pseudo Stokes' shifts (i.e. upon ligand excitation), and long luminescent lifetimes, in the microsecond range for near-infrared emitters and in the millisecond range for visible-emitting ions such as Eu^{III} or Tb^{III}; the latter feature allows time-gated detection with concomitant enhancement of the signal-to-noise ratio and very high sensitivity. Numerous applications in fields such as bio-analyses, bio-imaging and telecommunications are well documented.[1–3] The absorption coefficients of f-f transitions are extremely low, usually in the range 0.1–10 $M^{-1}\,cm^{-1}$, preventing efficient direct excitation and thus suitable sensitizing chromophores playing the role of antennae are required to efficiently populate the 4f excited states. Nowadays, one of the growing challenges in the design of lanthanide luminescent devices is to extend the excitation wavelength from the UV into the visible range of the electro-magnetic spectrum.[4] Indeed, excitation with energetic UV radiation, especially below 340 nm,[5] suffers severe drawbacks in the field of bio-analysis, since it generates significant auto-fluorescence, causes cell damage, and requires the use of costly quartz optics.

Presently, three different approaches are intensively explored with the aim of circumventing such undesired effect. The first one relies on multi-photon excitation of lanthanide complexes absorbing in the UV or visible range and displaying important multi-photon absorption cross-sections.[3,6–10] This technique presents the advantage of allowing excitation with near-infrared (NIR) light which is less absorbed by biological tissues and thus penetrates deeper into them; for instance, imaging depths of 500 μm are routinely obtained for brain tissues in this way.[11] On the other hand, powerful femto lasers are needed for achieving adequate excitation since multiphoton processes have very low probability. The second approach consists of the design of new sensitizer systems capable of strongly absorbing visible light and subsequently transfering energy onto the emitting lanthanide ions. Up to now, d-block chromophores are the most intensely investigated sensitizing groups taking advantage of their intense metal-to-ligand charge transfer absorption bands generally spanning the visible range.[12–17] The main disadvantages of such sensitizing systems are (i) the high prices of most of the adequate d-metals (mainly Cr^{III}, Ir^{III}, Os^{II}, Pt^{II}, Pd^{II}, Re^{I}, and Ru^{II}) and (ii) the large spatial distance *r* separating the donor and acceptor moieties, i.e. the absorbing d-block and the emissive lanthanide ion, that often reduces the efficiency of the energy transfer. Finally, it is also feasible to funnel energy through visible absorption bands (π-π* or intra-ligand charge transfer, ILCT) of purely organic chromophores such as fluorescein,[18] rhodamine,[19] 8-hydroxyquinoline,[20–22] carbazole-[4] or tetrazine-based[23] ligands, as well as boradiazaindacene dyes,[24] to name but a few examples. However, visible-absorbing organic chromophores with do-

[a] École Polytechnique Fédérale de Lausanne, Laboratory of Lanthanide Supramolecular Chemistry,
BCH-1405, 1015 Lausanne, Switzerland
[b] Korea University, Department of Advanced Materials Chemistry, WCU Center for Next Generation Photovoltaic Systems, Sejong Campus, Jochiwon, JungNam 339-700, South Korea
Supporting information for this article is available on the WWW under http://dx.doi.org/10.1002/ejic.200901148.

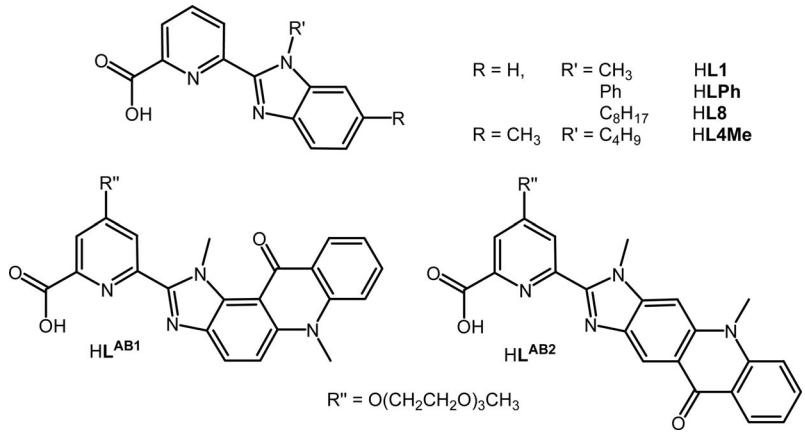

Scheme 1. Monotopic tridentate ligands with benzimidazole-substituted pyridine-2-carboxylic acid core.

nor levels compatible with a significant energy transfer to the $^5D_0$-excited level of Eu^{III} (> 17 300 cm^{-1}) or Tb^{III} (> 21 500 cm^{-1}) are rather rare. Among the few examples cited in the literature, which include [Eu(tta)$_3$(dpbt)] [tta = thenoyltrifluoroacetonate, dpbt = 2-(4-diethylaminophenyl)-4,6-bis(3,5-dimethylpyrazol-1-yl)-1,3,5-triazine],[25] polyaminocarboxylates with one pendant arm bearing a sensitizing acridone group,[26,27] [Eu(fod)$_3$(MK)] complex (MK = Michler's ketone, fod = 6,6,7,7,8,8,8-heptafluoro-2,2-dimethyl-3,5-dione),[28] and [Eu(PHN)$_3$(H_2O)(DMF)]-PHN (HPHN = 9-hydroxyphenal-1-one),[29] only the ternary complex prepared by Zhang's group[25] displays remarkable photophysical properties; the overall quantum yield amounts to 52% in toluene, this sizeable value being due to efficient energy transfer which, unusually, operates from a singlet state. All the other above-mentioned examples for which the energy transfer process involves triplet states of the ligands, have much lower overall quantum yields (0.5–17%).

Acridone, used as a tag in fluorescence-based assays,[30,31] has been grafted as a pendant arm on macrocyclic cyclen-based ligands by Faulkner's group[27] in order to sensitize Eu^{III} luminescence. Advantages of such a heterocycle include its chemical inertness, its remarkable resistance to photobleaching and, above all, the possibility to be excited around 400–420 nm. The idea underlying the present work is to incorporate such a sensitizing group into the skeleton of a benzimidazole-substituted pyridine-2-carboxylic acid. Tridentate ligands such as H**L1**, H**LPhe** or H**L4Me** (Scheme 1) yield nine-coordinate Eu^{III} complexes with sizeable quantum yields, as demonstrated recently in our group.[32] Similarly to most of the organic sensitizers reported to date, they however suffer from their UV excitation, around 320 nm, which restricts their potential uses. In a effort to overcome this limitation, we report here the synthesis of two new fused acridone-benzimidazole ligands HL^{AB1} and HL^{AB2} (Scheme 1) together with a detailed investigation of the thermodynamic stability and photophysical properties of some of their [Ln($\mathbf{L}^{ABX}$)$_3$] complexes (x = 1 or 2; Ln = La, Nd, Gd, Eu, Er, Yb) emitting either in the visible or in the NIR ranges.

Results and Discussion

Synthesis

The two ring-fused acridone-benzimidazole ligands HL^{ABX} (X = 1–2) were prepared according to the same 10-step synthetic pathway. The first part of the synthesis was dedicated to the formation of the suitable 10-methyl-*m*-(methylamino)-*n*-nitroacridin-9(10*H*)-one precursors $\mathbf{I_{17}}$ and $\mathbf{I_{27}}$ (Scheme 2).

The first step consists in a substitution of the fluoride atom in the *ortho*-position of the benzoic acid derivatives by sodium salts of the adequate aromatic amide generated in situ by reaction of the corresponding aniline derivatives with sodium amide.[33] It can be stressed that a minimum amount of three equivalents of base is required for the reaction going to completion since the product is rapidly deprotonated under such experimental conditions. The second step involves ring closure by a classical intramolecular Friedel–Crafts acylation with a mixture of phosphorus pentoxide and *ortho*-phosphoric acid.[34] Intermediate product $\mathbf{I_{22}}$ was obtained as a mixture of two isomers. In view of their poor solubility in common organic solvents, these two isomers were directly converted into their *N*-methyl analogues, similarly to $\mathbf{I_{12}}$, with an excess of methyl iodide in presence of sodium hydride. Mono-nitration of the *N*-methylacridone derivatives was conducted with a stoichiometric amount of nitric acid in acetic anhydride. Earlier synthetic studies have demonstrated that the regioselectivity of the nitration is affected by the previous *N*-methylation of acridone rings.[35] Indeed, such methylation increases the ratio between the desired *para* isomers (relative to the methylamino group) and the *ortho* isomers. Furthermore, the reaction preferentially takes place on the most electron-rich aromatic ring which bears the weakly electron-donating methoxy group. Finally, three more steps were needed to replace the methoxy group of intermediates $\mathbf{I_{14}}$ and $\mathbf{I_{24}}$ by a methylamino group. The C–O cleavage of the methoxy group was performed in presence of an excess of anhydrous aluminum chloride to afford the phenol derivatives.[34] In order to activate the carbon atom bearing the hydroxy

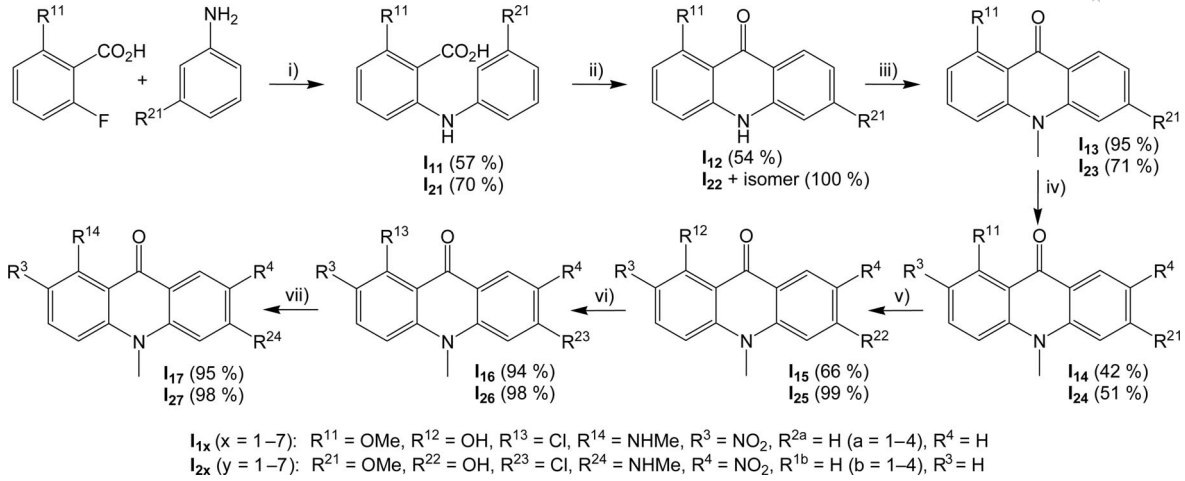

Scheme 2. Synthesis of the precursors $\mathbf{I_{1x}}$ and $\mathbf{I_{2x}}$ (x = 1–7): i) $NaNH_2$ (3.2 equiv.), THF (50 °C, 16 h); ii) P_2O_5, H_3PO_4 (110 °C, 16 h); iii) MeI (2.7 equiv.), NaH (2.75 equiv.), DMF (85 °C, 16 h); iv) HNO_3 (1.0 equiv.), Ac_2O (25 or 50 °C, 6 or 16 h); v) $AlCl_3$ (2.4 equiv.), $C_2H_4Cl_2$ (reflux, 2–3 h); vi) $POCl_3$, DMF (30 or 50 °C, 72 h); vii) $MeNH_2$ solution 2 M in THF (25 °C, 16 or 72 h).

group, different chlorinating agents, such as phosphorus oxychloride, phosphorus pentachloride and phenylphosphonic dichloride, were tested without success. Only dimethyl chloro-iminium chloride[36] generated in situ by reaction between phosphorus oxychloride and dry DMF at 30 °C, was enough reactive to achieve the conversion of the phenol groups into the corresponding chloro-arene derivatives in excellent yield. Then, easy substitution of the chloride atom by a methylamino group was performed in methylamine solution at room temperature to form the key intermediates $\mathbf{I_{17}}$ and $\mathbf{I_{27}}$.

The second part of the synthesis adopts the same route as those previously described for ligands $H_2\mathbf{L^{CX}}$ (X = 2, 4–6),[37,38] and is presented in Scheme 3. The key intermediate **1** was prepared in three steps from the commercially available chelidamic acid.[38] It bears a poly(oxyethylene) substituent in *para*-position of the pyridine ring which readily enhances the solubility of the last intermediates as well as of the final ligands in both aqueous and organic solvents. Intermediate **1** was then converted into the corresponding acid chloride and subsequently condensed with the adequate intermediate $\mathbf{I_{17}}$ or $\mathbf{I_{27}}$ by means of a modified Philips coupling reaction.[39] Contrary to the previous condensations achieved by our group, the reaction only occurs in refluxing dry toluene. Indeed, the *N*-methylaromatic amines used here are non reactive in refluxing dichloromethane as a direct consequence of their extremely poor nucleophilic character. The resulting amides $\mathbf{I_{18}}$ and $\mathbf{I_{28}}$ were reduced in presence of a large excess of iron to form the benzimidazole intermediates $\mathbf{I_{19}}$ and $\mathbf{I_{29}}$. Final hydrolysis of the monoethyl ester function led to the target ligands with overall yields [steps (i)–(xii) in Schemes 1 and 2] of 2 and 17% for $H\mathbf{L^{AB1}}$ and $H\mathbf{L^{AB2}}$, respectively.

Formation of the $[Ln(\mathbf{L^{ABX}})_3]$ Complexes in MeCN/MeOH

Attempts to form the $[Ln(\mathbf{L^{ABX}})_3]$ chelates in buffered aqueous solution (TRIS-HCl 0.1 M) were unsuccessful owing to the insolubility of the neutral 1:3 compounds: the hydrophobic acridone-benzimidazole shell around the metal ion is not enough counter-balanced by the presence of the water-soluble poly(oxyethylene) arms. The self-assembly process between the monotopic ligands and some lanthanide ions was consequently studied in organic solvents (acetonitrile or acetonitrile/methanol mixture) by two experimental techniques. Firstly, the 1:3 stoichiometric solutions of trivalent lanthanide ions (Ln = La, Eu and Yb) with ligands $(\mathbf{L^{ABX}})^-$ were characterized by ESI-TOF mass spectrometry in order to provide an insight into the nature of the metallic species present in solution. From the mass-spectrometric data recorded in acetonitrile/methanol (1:2, v/v) with a total ligand concentration of 9×10^{-4} M, the solutions with $(\mathbf{L^{AB1}})^-$ contain a single complex species with 1:3 (Ln:L) stoichiometry. The corresponding peaks are intense and are the base peaks in the case of Eu and Yb. The situation is quite different for $(\mathbf{L^{AB2}})^-$ solutions for which the base peak can be assigned to the free ligand. For Eu and Yb, very small peaks are seen which arise from the 1:3 complexes, while no such signal is recorded for La (see Table 1 and Tables S1–S2 in the Supporting Information). This highlights that the solvent efficiently compete with complex formation with this ligand and/or that important dissociation processes occur under the experimental conditions used. High resolution scans of the peaks attributed to $[Eu(\mathbf{L^{AB1}})_3]$ and $[Eu(\mathbf{L^{AB2}})_3]$ are shown in Figure 1 and the calculated isotopic distributions perfectly match the experimental ones.

Formation Constants of the $[Ln(\mathbf{L^{ABX}})_n]$ Complexes in MeCN

In view of the ES-MS data, spectrophotometric titrations were performed in neat acetonitrile in order to maximize complex formation. Solutions of ligands $(\mathbf{L^{ABX}})^-$ (1.43×10^{-5} M, $x = 1$; 2.00×10^{-5} M, $x = 2$) were titrated with concentrated solutions of lanthanide perchlorates (Ln = La,

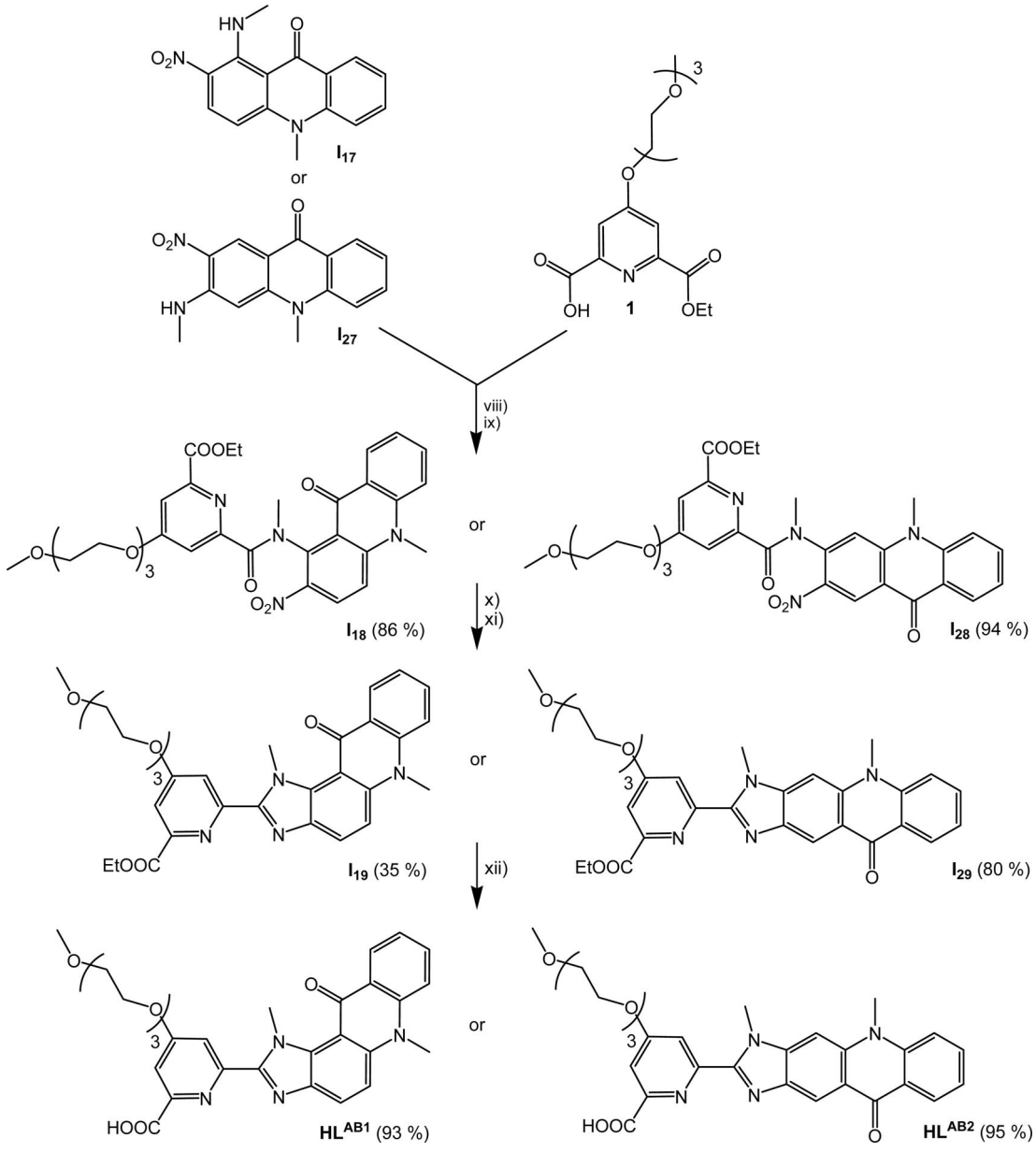

Scheme 3. Synthesis of the new monotopic ligands HL^{AB1} and HL^{AB2}: viii) $SOCl_2$ (10 equiv.), DMF (0.1 equiv.), 1 (2.3 or 2.8 equiv.), CH_2Cl_2 (reflux, 2 h); ix) $\mathbf{I_{17}}$ or $\mathbf{I_{27}}$ (1 equiv.), NEt_3, toluene (reflux, overnight); x) Fe^0 (15 equiv., EtOH/H_2O/HCl (reflux, overnight); xi) EtOH/H_2SO_4 (reflux, 4 h or overnight); xii) NaOH (1.5 equiv.), EtOH (25 °C, 16 h).

Table 1. Major peaks corresponding to Ln-containing species found in the ESI-TOF spectra of 1:3 Ln/$(\mathbf{L^{ABX}})^-$ stoichiometric solutions in acetonitrile/methanol (1:2, v/v) with a total ligand concentration of 9×10^{-4} M.

Species	*m/z* (obsd.)	Intensity[a]	Assignment	*m/z* (calcd.)	MW [Da][b]
$[La(\mathbf{L^{AB1}})_3]$[c]	910.86	40	$[M + 2\ Na]^{2+}/2$	910.80	1775.63
$[Eu(\mathbf{L^{AB1}})_3]$	917.10	100	$[M + 2\ Na]^{2+}/2$	917.32	1788.67
$[Yb(\mathbf{L^{AB1}})_3]$	927.97	100	$[M + 2\ Na]^{2+}/2$	927.86	1809.75
$[La(\mathbf{L^{AB2}})_3]$[c]	n.a.	n.a.	n.a.	n.a.	1775.63
$[Eu(\mathbf{L^{AB2}})_3]$[c]	895.55	≤2	$[M + 2\ H]^{2+}/2$	895.34	1788.67
$[Yb(\mathbf{L^{AB2}})_3]$[c]	916.31	≤1	$[M + H + Na]^{2+}/2$	916.86	1809.75

[a] In percentage of the base peak. [b] Molecular weight of the parent species. [c] Peak $[L + H]^+$ of the ligand $\mathbf{HL^{ABX}}$ observed as base peak at *m/z* = 547.24.

Eu, Yb, ca. 5×10^{-3} M) for ratios $R = [Ln]_t/[(\mathbf{L^{ABX}})^-]_t$ ranging from 0 to 4 in order to determine the stability constants of the successive complexes formed. The experiments were conducted under nitrogen atmosphere so as to keep water concentration as low as possible. After completion of the titration, the water content of the La and Eu solutions was

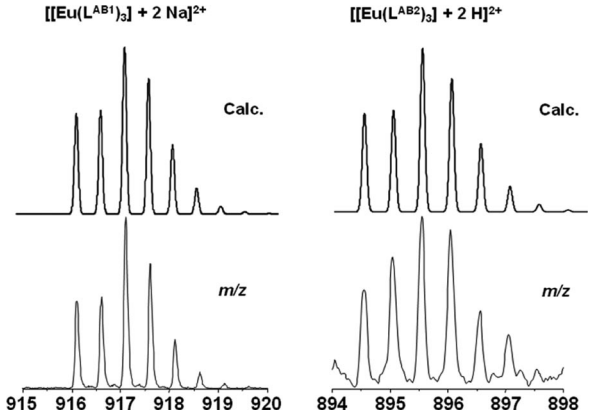

Figure 1. Experimental and calculated isotopic distributions of the signals assigned to $[Eu(\mathbf{L}^{\mathbf{ABX}})_3]$ in MeCN/MeOH 1:2 v/v.

determined by Karl-Fischer method and corresponded to an average value of 240 ppm for solutions with ligand $(\mathbf{L}^{\mathbf{AB2}})^-$.

Factor analysis pointed to the presence of 4–5 absorbing species in solution (i.e. with eigenvectors $>10^{-2}$) and several models were tested for the least-squares fit of the data. The best convergences were reached and smallest residuals were obtained when 1:1, 1:2 and 1:3 complexes were introduced into the models in addition to the free ligand. Introduction of additional species such as 2:1 or 2:2 complexes as well as removal of one of the previously mentioned species, invariably led to non-convergence of the fitting procedure. Therefore the following model was retained; see Equations (1), (2), and (3), charges are omitted for clarity reasons.

$$\mathbf{L}^{\mathbf{ABX}} + Ln \leftrightarrows [Ln(\mathbf{L}^{\mathbf{ABX}})_1] \qquad \log\beta_{11} \qquad (1)$$

$$2\ \mathbf{L}^{\mathbf{ABX}} + Ln \leftrightarrows [Ln(\mathbf{L}^{\mathbf{ABX}})_2] \qquad \log\beta_{12} \qquad (2)$$

$$3\ \mathbf{L}^{\mathbf{ABX}} + Ln \leftrightarrows [Ln(\mathbf{L}^{\mathbf{ABX}})_3] \qquad \log\beta_{13} \qquad (3)$$

The corresponding overall stability constants are listed in Table 2 along those determined for two analogous tridentate ligands, namely **L1** and **L2**, under similar experimental conditions (Scheme 4).[40] The distribution diagram of the Eu/$(\mathbf{L}^{\mathbf{AB1}})^-$ system reproduced on Figure 2 clearly shows the preferential formation of one major complex species at stoichiometric ratio $R = 0.33$ (86% of the total ligand concentration). The other distribution diagrams, along with the evolution of the absorption spectra during the titrations are depicted on Figures S1–S6 (Supporting Information).

The recalculated spectra of the various species displayed on Figures S7–S8 (Supporting Information) are strongly correlated so that interpretation of the cumulative stability constants listed in Table 2 must be done with some care. However, some general trends can be outlined:

(i) The carboxylic acid group of the ligands plays a predominant role in the thermodynamic stability of the $[Ln(\mathbf{L}^{\mathbf{ABX}})_3]$ complexes, as previously observed for binuclear triple-stranded helicates:[41] Indeed, the conditional stability constants of the mononuclear 1:3 species are between 4 and 8 orders of magnitude larger than those found for the corresponding complexes with **L2**.

Table 2. Conditional stability constants determined by spectrophotometric titrations in MeCN at room temperature with standard deviations between parentheses.

Ligand		La	Eu	Gd	Yb	Lu
$(\mathbf{L}^{\mathbf{AB1}})^-$	$\log\beta_{11}$	8.9(4)	9.4(1)	n.a.	9.9(2)	n.a.
	$\log\beta_{12}$	15.7(5)	17.3(1)	n.a.	17.5(2)	n.a.
	$\log\beta_{13}$	22.8(7)	24.6(2)	n.a.	25.3(3)	n.a.
$(\mathbf{L}^{\mathbf{AB2}})^-$	$\log\beta_{11}$	8.6(1)	8.2(1)	n.a.	9.3(4)	n.a.
	$\log\beta_{12}$	15.4(1)	15.0(1)	n.a.	17.1(6)	n.a.
	$\log\beta_{13}$	22.5(2)	21.8(2)	n.a.	23.3(8)	n.a.
L1[a]	$\log\beta_{11}$	8.9(3)	9.0(2)	n.a.	9.4(5)	n.a.
	$\log\beta_{12}$	16.8(8)	15.7(7)	n.a.	16.5(1)	n.a.
	$\log\beta_{13}$	22.6(9)	22.6(6)	n.a.	19.9(1)	n.a.
L2[a]	$\log\beta_{11}$	7.1(3)	n.a.	7.3(2)	n.a.	7.2(2)
	$\log\beta_{12}$	11.6(4)	n.a.	12.3(3)	n.a.	11.5(4)
	$\log\beta_{13}$	15.9(5)	n.a.	17.4(4)	n.a.	17.3(4)

[a] From reference.[40]

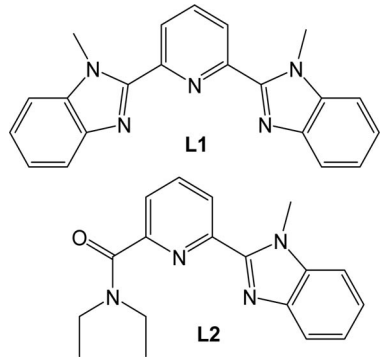

Scheme 4. Tridentate ligands used for comparison purposes.

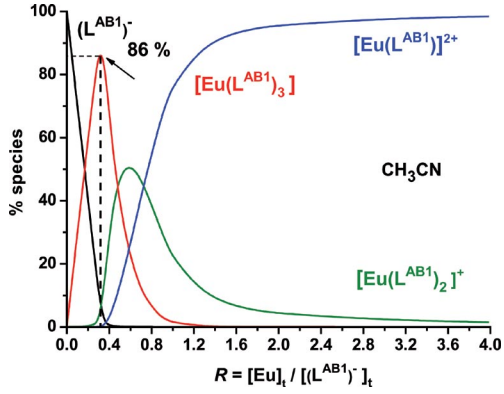

Figure 2. Distribution diagram of the $Eu^{III}/(L^{AB1})^-$ system in acetonitrile computed with the conditional stability constants reported in Table 2; $[(\mathbf{L}^{\mathbf{AB1}})^-]_t = 1.43 \times 10^{-5}$ M.

(ii) The 1:3 complexes between ligands $(\mathbf{L}^{\mathbf{ABX}})^-$ and the heavier lanthanide ions (Eu, Yb) are more stable than those with ligand **L1** while the La complexes have comparable stability; this may be ascribed to the contraction of the ligand coordinating pocket in going from **L1** to $(\mathbf{L}^{\mathbf{ABX}})^-$ which therefore provides a tighter binding to the smallest lanthanide ions; this assumption is supported by a previous study involving **L1** which demonstrated that such a ligand preferentially binds the larger lanthanide ions over the smaller ones;[42] in addition the weakly electron-donating

flexible arm in the *para*-position of the pyridine heterocycle may also contribute to the enhanced stability of the $[Ln(\mathbf{L}^{\mathbf{ABX}})_3]$ complexes.

(iii) The $[Ln(\mathbf{L}^{\mathbf{AB1}})_3]$ chelates (Ln = Eu, Yb) exhibit a somewhat larger stability compared to the complexes with $(\mathbf{L}^{\mathbf{AB2}})^-$. No obvious interpretation of this last observation can be done although possible discrepancy in the flattening of the ligands $(\mathbf{L}^{\mathbf{ABX}})^-$ and interstrand π-stacking interactions inside the complexes could be invoked. Unfortunately, as for the previously reported binuclear helicates bearing polyoxyethylene arms,[38,43] no single crystals suitable for X-ray analysis could be grown, most probably in view of the presence of the three fluxional pendants so that this assumption could not be proven.

^{1}H NMR spectra of stoichiometric 1:3 solutions of Lu^{III} and $(\mathbf{L}^{\mathbf{ABX}})^-$ were also recorded in CD_2Cl_2 or $CDCl_3$ at various temperatures but any interpretation of the best-resolved spectra is precluded due to the presence of two strongly overlapping sets of signals observed in both aliphatic and aromatic regions. This may be traced back to the self-assembly of the non-symmetric ligands with lanthanide ions giving rise to at least two isomers, namely *fac*-$[Ln(\mathbf{L}^{\mathbf{ABX}})_3]$ and *mer*-$[Ln(\mathbf{L}^{\mathbf{ABX}})_3]$ complexes[44] which generate up to 24 resonances in the aromatic region (that is three times more than the eight non-equivalent aromatic protons of the ligands). Furthermore, the presence of additional minor species such as the 1:2 species and the free ligand (see Figure 2) cannot be excluded.

Ligand-Centred Photophysical Data

The UV/Vis absorption spectra of the deprotonated ligands $(\mathbf{L}^{\mathbf{ABX}})^-$ and some of their 1:3 complexes were recorded in neat acetonitrile at room temperature (Figure 3, Figure S9 in the Supporting Information). Their main spectral features are summarized in Table 3.

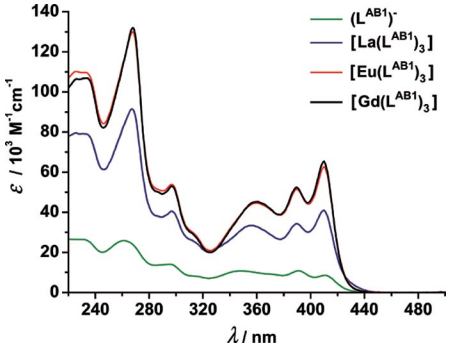

Figure 3. Absorption spectra of the ligand $(\mathbf{L}^{\mathbf{AB1}})^-$ and some of its 1:3 complexes in neat acetonitrile, $[(\mathbf{L}^{\mathbf{AB1}})^-]_t = 2.25 \times 10^{-5}$ M.

The spectra of deprotonated ligands $(\mathbf{L}^{\mathbf{ABX}})^-$ display 4–5 absorption bands in the range 250–440 nm. Upon complexation with Ln^{III} ions, the three most energetic transitions of $(\mathbf{L}^{\mathbf{AB1}})^-$ are moderately red shifted from 250 up to 1050 cm^{-1}. In the case of ligand $(\mathbf{L}^{\mathbf{AB2}})^-$, the effects of the complexation are less pronounced since the energies of corresponding electronic transitions have a maximal shift of only 250 cm^{-1}. The two less energetic transitions, around 380–420 nm for $(\mathbf{L}^{\mathbf{AB1}})^-$ and 400–450 nm for $(\mathbf{L}^{\mathbf{AB2}})^-$, are hardly affected by the complexation and can therefore be assigned to π→π* transitions with a marked charge-transfer character, mainly originated from *N*-methylacridone moiety, with typical log ε values of 3.9–4.0.

Table 3. Ligand-centred electronic transitions of the deprotonated ligands and their complexes in neat acetonitrile at room temperature: energy[a] in cm^{-1} and log ε values between parentheses.

Species	E_1(*π←π) (log ε)	E_2(*π←π) (log ε)	E_3(*π←π) (log ε)	E_4(*π←π) (log ε)	E_5(*π←π) (log ε)
$(\mathbf{L}^{\mathbf{AB1}})^-$	38250 (4.41)	33900 (4.15)	28800 (4.03)	25600 (4.03)	24350 (3.93)
$[La(\mathbf{L}^{\mathbf{AB1}})_3]$	37450 (4.96)	33650 (4.61)	28100 (4.53)	25650 (4.54)	24400 (4.61)
$[Eu(\mathbf{L}^{\mathbf{AB1}})_3]$	37300 (5.11)	33650 (4.73)	27800 (4.65)	25650 (4.71)	24400 (4.80)
$[Gd(\mathbf{L}^{\mathbf{AB1}})_3]$	37300 (5.12)	33650 (4.72)	27750 (4.66)	25650 (4.72)	24400 (4.82)
$(\mathbf{L}^{\mathbf{AB2}})^-$	36250 (4.59)	31350 (4.55)	24350 (3.92)	23300 (4.04)	–
$[La(\mathbf{L}^{\mathbf{AB2}})_3]$	36250 (5.09)	31200 (4.98)	24450 (4.35)	23250 (4.47)	–
$[Gd(\mathbf{L}^{\mathbf{AB2}})_3]$	36150 (5.08)	31100 (4.99)	24300 (4.37)	23200 (4.49)	–
$[Yb(\mathbf{L}^{\mathbf{AB2}})_3]$	36250 (5.11)	31150 (5.01)	24400 (4.37)	23250 (4.50)	–

[a] Maxima of the band envelopes.

Upon excitation into their less energetic absorption bands, both ligands emit a broad band in the range 400–600 nm with maxima around 445 nm for $(\mathbf{L}^{\mathbf{AB1}})^-$ and 470 nm for $(\mathbf{L}^{\mathbf{AB2}})^-$ (Figure 4, Figures S10–S11 in the Supporting Information).

These bands disappear upon enforcement of a 50-μs time delay and are therefore assigned to fluorescence of the ligands. At 77 K, time-gated luminescence spectra display faint and broad phosphorescence bands extending from 500

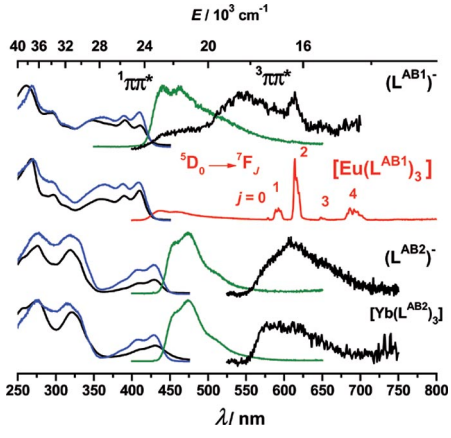

Figure 4. Left: normalized absorption (blue lines) and excitation (black lines) spectra of $(\mathbf{L}^{\mathbf{AB1}})^-$, $(\mathbf{L}^{\mathbf{AB2}})^-$, $[Eu(\mathbf{L}^{\mathbf{AB1}})_3]$ and $[Yb(\mathbf{L}^{\mathbf{AB2}})_3]$ measured in neat acetonitrile at 295 K. Right: normalized emission spectra of the same samples under excitation at 410.5–429.0 nm (ligands) and 410.0–430.5 nm (complexes); the triplet state emission (green lines) has been recorded at 77 K with a 50-μs time delay; other emissions have been recorded at 295 K without time-delay. $[(\mathbf{L}^{\mathbf{AB1}})^-]_t = 2.25 \times 10^{-5}$ M, $[(\mathbf{L}^{\mathbf{AB2}})^-]_t = 2.00 \times 10^{-5}$ M.

Table 4. Photophysical properties of the deprotonated ligands $(\mathbf{L^{ABX}})^-$ and their La^{III} and Gd^{III} complexes in neat acetonitrile at 77 or 295 K.

Species	E ($^1\pi\pi^*$) [cm^{-1}][a]	E ($^3\pi\pi^*$) [cm^{-1}][b]	τ ($^3\pi\pi^*$) [ms][c]	ΔE_0 [cm^{-1}][d]
$(\mathbf{L^{AB1}})^-$	22 450, 23 250	17 050, 18 100	520(40)	5400
$[La(\mathbf{L^{AB1}})_3]$	22 450, 23 300	17 550, 18 350	496(94)	4900
$[Gd(\mathbf{L^{AB1}})_3]$	22 450, 23 350	17 450, 18 450	4.15(7)	5000
$(\mathbf{L^{AB2}})^-$	21 200, 22 400	16 400, n.a.	n.a.	4800
$[La(\mathbf{L^{AB2}})_3]$	20 750, n.a.	15 350, 16 400	214(30)	5400
$[Gd(\mathbf{L^{AB2}})_3]$	21 100, 22 300	15 150, 16 450	19(1), 2.8(4)	5950

[a] From fluorescence spectra at 295 K, 0-phonon transition and maximum of the band envelope, λ_{exc} = 410.5 nm, $(\mathbf{L^{AB1}})^-$, or 429.0 nm, $(\mathbf{L^{AB2}})^-$, and 410.0, 430.5–431.0 nm for the corresponding complexes. [b] From phosphorescence spectra at 77 K, 0-phonon transition and maximum of the band envelope, same λ_{exc} as for fluorescence spectra. [c] At 77 K. [d] $\Delta E_0 = E_0(^3\pi\pi^*) - E_0(^1\pi\pi^*)$.

to 720 nm with maxima around 590 nm for $(\mathbf{L^{AB1}})^-$ and 610 nm for $(\mathbf{L^{AB2}})^-$; a long lifetime of 520 ms is measured for $(\mathbf{L^{AB1}})^-$ while the phosphorescence of the second ligand is too weak to obtain reliable data. Both singlet and triplet energy levels of the ligand $(\mathbf{L^{AB1}})^-$ remain almost unchanged upon complexation with non-luminescent Ln^{III} ions (Ln = La, Gd) with variations in the range of $\pm 400\ cm^{-1}$ (Figures S10–S11 in the Supporting Information). The triplet state levels of non-luminescent complexes of $(\mathbf{L^{AB2}})^-$ are significantly red shifted by about 1200 cm^{-1} whereas the singlet state energies are less affected ($\pm$ 450 cm^{-1}). The energy gaps ΔE_0 between both ligand levels inside the complexes are within or slightly above the ideal range of values (4000–5000 cm^{-1}) generally accepted for efficient intersystem-crossing (Table 4) which often plays a major role in the overall ligand-to-metal energy-transfer process.[3]

Both Gd^{III} complexes have short phosphorescence lifetimes due to the heavy atom effect generated by the paramagnetic ion (S = 7/2).[45] For the $[Gd(\mathbf{L^{AB1}})_3]$ complex, a single lifetime of 4.15 ms was found whereas two different lifetimes of 19 (population ca. 57%) and 2.8 ms (population ca. 43%) were obtained in the case of the $[Gd(\mathbf{L^{AB2}})_3]$ complex. Though the energy gap $E_0(^3\pi\pi^*) - E(^5D_0)$ lies in a optimal range of values, an important residual fluorescence of the ligand (67% of the total fluorescence intensity of the free ligand) was observed in the emission spectrum of the $[Eu(\mathbf{L^{AB1}})_3]$ complex recorded at room temperature. This observation tends to prove that both fluorescence and intersystem-crossing rate constants are relatively similar ($k_{fluor} \approx k_{isc}$) so that such a system is not completely optimum in terms of singlet-to-triplet energy conversion. It is however noteworthy that part of this residual fluorescence originates from the dissociated ligand present in solution. Indeed, the formation of the 1:3 species is not quantitative (about 86%, see Figure 2) at this concentration in neat acetonitrile.

Regarding the ability of both ligands to sensitize Ln^{III} luminescence, we anticipate that $(\mathbf{L^{AB1}})^-$ is better suited for transferring energy onto the visible-emitting Eu^{III} ion ($^5D_0$ $\approx$ 17300 cm^{-1}) whereas $(\mathbf{L^{AB2}})^-$ is more adapted for the near-infrared emission of Nd^{III} ($^4F_{3/2} \approx 11300\ cm^{-1}$), Er^{III} ($^4I_{13/2} \approx 6500\ cm^{-1}$) and Yb^{III} ($^2F_{5/2} \approx 10200\ cm^{-1}$) as a direct consequence of the respective 0-phonon energy levels of the triplet states {ca. 18400 and 16400 cm^{-1} for $[Ln(\mathbf{L^{AB1}})_3]$ and $[Ln(\mathbf{L^{AB2}})_3]$, respectively} and assuming that the triplet states are the main donor levels transferring energy onto the lanthanide ions. Sensitization of Eu^{III} and Yb^{III} luminescence is proved by the close match between the absorption and excitation spectra (Figure 4).

Photophysical Properties of $[Eu(\mathbf{L^{AB1}})_3]$

Emission spectra of the $[Eu(\mathbf{L^{AB1}})_3]$ complex were recorded in both neat acetonitrile solution at 295 K (Figure 4) and frozen acetonitrile solution at 10 K by means of a high-resolution laser setup (Figure 5) in the latter case. The spectra are dominated by the hypersensitive $^5D_0 \rightarrow {}^7F_2$ transition; lowering the temperature does not alter the relative intensities of the Eu^{III} emission lines but leads to typical line narrowing due to the removal of the vibronic contributions.[46] To gain additional information about the inner coordination sphere of the Eu^{III} ion, analysis of both $^5D_0 \rightarrow {}^7F_0$ and $^5D_0 \rightarrow {}^7F_1$ transitions was carried out on the high-resolution spectrum recorded at 10 K (Figure 5). The $^5D_0 \rightarrow {}^7F_0$ transition is weak (0.6% of the total $^5D_0$ emission), broad (full-width-at half-height: 29 cm^{-1}), and slightly asymmetric on its high-energy side; this could be

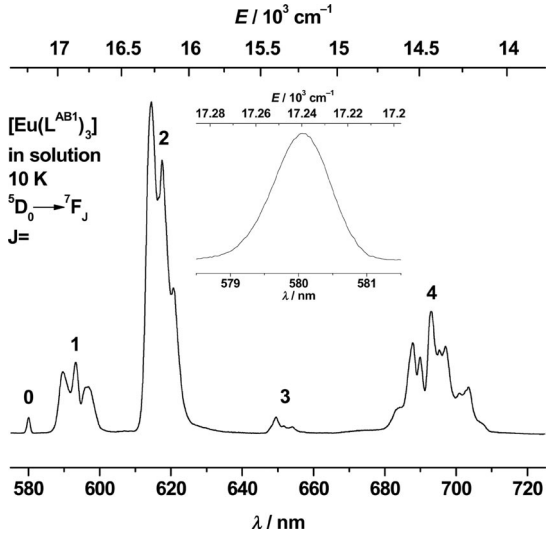

Figure 5. High-resolution emission spectrum of the $[Eu(\mathbf{L^{AB1}})_3]$ complex in frozen acetonitrile recorded at 10 K, λ_{exc} = 420 nm. Insert: detail of the $^5D_0 \rightarrow {}^7F_0$ transition; $[(\mathbf{L^{AB1}})^-]_t = 2.25 \times 10^{-5}$ M.

indicative of the presence of a second minor species in solution. Furthermore, the energy of the major component, 17238 cm^{-1} matches reasonably well the theoretical value for a N_6O_3 environment (17231 cm^{-1}) calculated from a phenomenological equation[47] with the following nephelauxetic parameters: $\delta_{carb} = -17.2$ cm^{-1} for the carboxylates and $\delta_{bzp} = -15.3$ cm^{-1} for the heterocyclic nitrogen donors.[48] The $^5D_0 \rightarrow {}^7F_1$ transition is split into three almost equally spaced component (ΔE = 106 and 104 cm^{-1}) and having approximately the same energy. This precludes an analysis in terms of pseudo D_3 symmetry similar to the one carried out for similar N_6O_3 environments in binuclear helicates[2,38] and points to a low symmetry environment for the metal ion (C_{2v} or lower). The important distortion from the idealized tricapped trigonal prismatic geometry often seen in nine-coordinate chelates is possibly induced by the steric hindrance between the bulky *N*-methylacridone moieties of two neighboring ligands.

The luminescence decays of the [Eu($\mathbf{L}^{\mathbf{AB1}}$)$_3$] solution are a monoexponential function (0.93 ± 0.01 ms) in solution at room temperature and a bi-exponential one at 10 K in frozen acetonitrile with corresponding lifetimes equal to 1.92 ± 0.02 ms (population ca. 84%) and 0.34 ± 0.03 ms (population ca. 16%). This reflects the presence of two different species in solution which are in fast exchange at room temperature. We note that the proportion of the species with the longest lifetime corresponds exactly to the speciation of the 1:3 complex found by spectrophotometric titration (see Figure 2). The long lifetime is evidence for the inner coordination sphere being devoid of water molecules. As a comparison, the Eu($^5D_0$) lifetime of [Eu($\mathbf{L2}$)$_3$]$^{3+}$ amounts to 1.98 ms in acetonitrile at room temperature,[40] while the one of the neutral chelate [Eu($\mathbf{L8}$)$_3$] (Scheme 1) is longer, 2.76 ms in dichloromethane. The other species are hydrated, with 2–3 water molecules in the inner coordination sphere. The large temperature dependence of the lifetime points to back energy transfer being operative (see below) and/or to the presence of a photoelectron transfer phenomenon, similar to the one evidenced for [Eu($\mathbf{L1}$)$_3$]$^{3+}$.[49,50]

At room temperature, a quantum yield of 10% was found for the solution in acetonitrile. Taking into account the speciation, this corresponds to a quantum yield of about 11.5% for the tris complex. This value is sizeable given the small energy gap, $\Delta E[^3\pi\pi^*(0)\text{-}^5D_0] \approx 1100$ cm^{-1}, which reduces the luminescence sensitization by allowing back transfer, as indicated by the temperature dependence of the Eu($^5D_0$) lifetime. A quantity of interest, when it comes to design ligands able to generate efficient antenna effects, is the sensitization efficiency η_{sens} which can be deduced from two experimentally accessible parameters, the overall quantum yield Q^L_{Ln} (i.e. upon excitation in the ligand electronic levels) and the intrinsic quantum yield Q^{Ln}_{Ln} (i.e., upon direct f-f excitation); see Equation (4).

$$\eta_{sens} = Q^L_{Ln}/Q^{Ln}_{Ln} \quad (4)$$

Since Q^{Ln}_{Ln} is difficult to determine experimentally owing to the small oscillator strength of the f-f transitions, it is usually estimated from the radiative lifetime, τ_{rad}, itself calculated from the Eu^{III} emission spectrum; see Equations (5) and (6).[3]

$$Q^{Ln}_{Ln} = \tau_{obs}/\tau_{rad} \quad (5)$$

$$1/\tau_{rad} = A_{MD,0} \times n^3 \times (I_{tot}/I_{MD}) \quad (6)$$

where $A_{MD,0}$ is the emission probability of the magnetic dipole transition $^5D_0 \rightarrow {}^7F_1$ (14.65 s^{-1}), n the refractive index (1.344 for acetonitrile), and I_{tot} and I_{MD} are the corrected integrated total emission intensity and intensity of the magnetic dipole transition, respectively. The calculated radiative lifetime for the solution is 4.0 ± 0.4 ms, a value comparable to those recently published for a series of analogous 1:3 complexes (4.2–4.7 ms).[32] The resulting intrinsic quantum yield Q^{Eu}_{Eu} appears to be small, only 23 ± 3%, but this value is certainly largely underestimated in view of the short lifetime consecutive to back transfer. Therefore the evaluated sensitization efficiency of ($\mathbf{L}^{\mathbf{AB1}}$)$^-$, 50 ± 9%, has to be considered as being a lower estimate.

Photophysical Properties of the [Ln($\mathbf{L}^{\mathbf{AB2}}$)$_3$] Complexes

As stated above, the ligand ($\mathbf{L}^{\mathbf{AB2}}$)$^-$ appears to be well suited for sensitizing the luminescence of NIR-emitting Ln^{III} ions but not of Eu^{III}. This is confirmed by the absence of characteristic Eu-emission lines on the luminescence spectrum of the [Eu($\mathbf{L}^{\mathbf{AB2}}$)$_3$] complex recorded at 295 K; only very faint emission lines could be observed at 77 K (Figure S11 in the Supporting Information). On the other hand, complexes with Ln = Nd, Er, and Yb give rise to the characteristic NIR emission lines of these ions (Figure 6). In order to unravel the role played by solvent molecules in non-radiative de-activation of the metal ions, we have measured their luminescence lifetimes τ_{obs} and overall quantum yields Q^L_{Ln} in both non-deuterated and deuterated acetonitrile (Table 5).

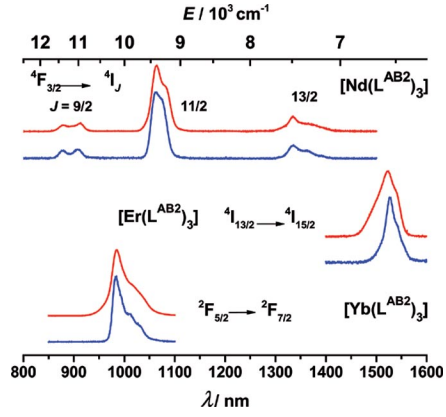

Figure 6. Normalized emission spectra of the Nd (top), Er (middle) and Yb (bottom) complexes of ligand ($\mathbf{L}^{\mathbf{AB2}}$)$^-$, at 295 K (red lines) and emission spectra of the same complexes at 77 K, without time-delay (blue lines), neat CH_3CN, λ_{exc} = 430.5–432.0 nm, [($\mathbf{L}^{\mathbf{AB2}}$)$^-$]$_{tot}$ = 2 × 10^{-5} M.

Table 5. Luminescent lifetimes τ_{obs} and overall quantum yields Q^{L}_{Ln} of solutions of the $[Ln(\mathbf{L^{AB2}})_3]$ complexes 7.5×10^{-5} M in non-deuterated and deuterated acetonitrile at 295 K. Standard deviations (2σ) are given between parentheses.

Species	$\tau_{obsd.}$ [μs][a] in CH_3CN	$\tau_{obsd.}$ [μs][a] in CD_3CN	Q^{L}_{Ln} [%][b] in CH_3CN	Q^{L}_{Ln} [%][b] in CD_3CN
$[Nd(L^{AB2})_3]$	12.0(7)	18.7(1)	0.16(1)	0.21(2)
$[Er(L^{AB2})_3]$	3.7(2)	4.03(1)	0.026(3)	0.030(3)
$[Yb(L^{AB2})_3]$	29.3(2)	33.5(4)	0.86(5)	1.2(1)

[a] Excitation wavelength: λ_{exc} = 355 nm. [b] Excitation wavelength: λ_{exc} = 430 nm.

All the measured luminescent decays were found to be monoexponential functions. In the case of Yb^{III}, the luminescence lifetime measured in the non-deuterated solvent (29.3 μs) is one of the longest reported to date in organic solution.[1,51,52,53–55] It only marginally increases in the deuterated solvent (33.5 μs). A similar trend is observed for the Er^{III} complex while the luminescent lifetime of the Nd^{III} complex is more affected by the deuteration of the solvent, increasing by about 30%. Overall quantum yield data are in good correlation with lifetime data in both solvents and values for Nd and Er lie in the standard range; on the other hand, the $[Yb(\mathbf{L^{AB2}})_3]$ solution displays a larger than usual quantum yield. We have estimated the sensitization efficiency of the ligand for the Yb^{III} luminescence by calculating the radiative lifetime from the $^2F_{5/2} \leftarrow {}^2F_{7/2}$ absorption spectrum; see Equation (7).[56]

$$\frac{1}{\tau_{rad}} = 2303 \times \frac{8\pi c n^2 \tilde{\nu}_m^{\,2}(2J+1)}{N_A(2J'+1)} \int \varepsilon(\tilde{\nu}) d\tilde{\nu} \qquad \tilde{\nu}_m = \frac{\int \tilde{\nu} \cdot \varepsilon(\tilde{\nu}) d\tilde{\nu}}{\int \varepsilon(\tilde{\nu}) d\tilde{\nu}} \tag{7}$$

where c is the speed of light in cm s^{-1}, N_A is Avogadro's number, J and J' are the quantum numbers for the ground and excited states, respectively, $\int\varepsilon(\tilde{\nu})d\tilde{\nu}$ is the integrated spectrum of the f-f transition, $\tilde{\nu}_m$ is the barycenter of the transition and n is the refractive index. A solid sample of the $[Yb(\mathbf{L^{AB2}})_3]$ complex was dissolved in chloroform/methanol (9:1) for solubility reasons. Its spectrum is displayed on Figure 7 and shows a maximum at 978 nm (10 225 cm^{-1}, ε = 5.2 M^{-1} cm^{-1}). Implementing $\tilde{\nu}_m$ = 10 333 cm^{-1}, n = 1.4356 and the relevant constants and integrals in Equation (7) yields a radiative lifetime of 900 ± 90 μs (Table 6). This value once again confirms that it is erroneous to assume a radiative lifetime of 2 ms when estimating the intrinsic quantum yields of Yb^{III} complexes in solution from Equation (5);[1] experimental reported values to date are in the range 0.51 to 1.3 ms[55–57] and the present value falls in the middle of this range. Corresponding data have also been determined for the $[Yb(\mathbf{L^{AB2}})_3]$ solid state sample. Both the $Yb(^2F_{5/2})$ lifetime and overall quantum yield are larger than in $CHCl_3$/MeOH solution by about 50%, which can be explained by the presence of closely diffusing OH vibrators quenching the luminescence in solution.[58] The radiative lifetime reported in Table 6 has been calculated from the solution lifetime by adjusting the refractive index (1.5 for a solid complex).[55] The intrinsic quantum yields of a few percents reflect efficient non-radiative de-activation processes due to the small energy difference between the emitting and the ground states. On the other hand, the sensitization efficiency of the ligand, $\eta_{sens} \approx$ 50–60%, is reasonably good. In view of the important residual fluorescence observed while extremely weak phosphorescence is seen under time-gated conditions (see Figure 4), one may infer that most of the energy loss occurs in the intersystem crossing and that if the triplet state is the main energy donor, the triplet-to-Yb^{III} transfer is quite efficient.

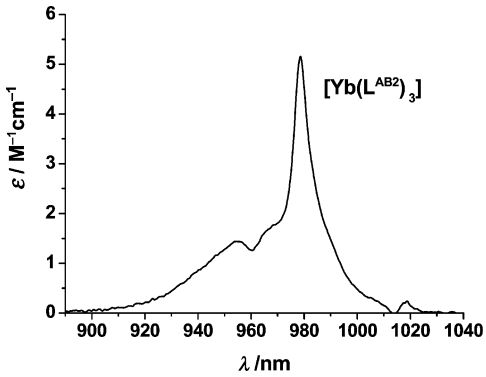

Figure 7. $Yb(^2F_{5/2} \leftarrow {}^2F_{7/2})$ absorption spectrum of a solution of $[Yb(\mathbf{L^{AB2}})_3]$ 3.51×10^{-3} M in chloroform/methanol (9:1, v/v) at 295 K.

Table 6. Photophysical parameters of a solution of $[Yb(\mathbf{L^{AB2}})_3]$ 3.51×10^{-3} M in chloroform/methanol (9:1, v/v) and in solid state at 295 K.[a]

	τ_{obs} [μs][b]	τ_{rad} [μs]	Q^{L}_{Yb} [%][c]	Q^{Yb}_{Yb} [%]	η_{sens} [%]
$CHCl_3$/MeOH, 9:1	16.5(0.1)	900	1.1(0.1)	1.8	61
Solid	24.8(0.1)	830	1.6(0.1)	3.0	54

[a] Standard deviations (2σ) between parentheses; speciation not taken into account; estimated relative errors (solution): τ_{obs}, ± 2%; τ_{rad}, ± 10%; Q^{L}_{Yb}, ± 10%; Q^{Yb}_{Yb}, ± 12%; η_{sens}, ± 22%. [b] λ_{exc} = 355 nm. [c] λ_{exc} = 430 nm.

Conclusions

Incorporation of a *N*-methylacridone heterocycle into the skeleton of previously described *N*-methylbenzimidazole pyridine-2-carboxylic acid ligands has been successfully achieved according to a unique synthetic route leading to ligands $H\mathbf{L^{AB1}}$ and $H\mathbf{L^{AB2}}$, thus considerably extending the range of applications of this tridentate framework. Both deprotonated ligands $(\mathbf{L^{ABX}})^-$ self-assemble with lanthanide ions to form neutral stable $[Ln(\mathbf{L^{ABX}})_3]$ complexes ($\log\beta_{13} \approx$

22–25) under stoichiometric conditions. Photophysical data highlight the degree of electronic tuning provided by the grafting of the acridone moiety at different positions of the benzimidazole: ligand $(\mathbf{L^{AB1}})^-$, with $E[^3\pi\pi^*(0)] \approx 18\,450\ cm^{-1}$ is a relatively good sensitizer of the Eu^{III} luminescence despite the presence of non-radiative back-transfer de-activation while ligand $(\mathbf{L^{AB2}})^-$, with a triplet state energy of about $16\,450\ cm^{-1}$, is a good sensitizer of the NIR-emitting Ln^{III}, particularly of Yb^{III}, although to a lesser extent than 8-hydroxyquinolinate (60 vs. about 100%).[55] The main energy losses incurred in the complex energy transfer process between the ligand and the metal ion seem to arise from a not optimum yield of intersystem crossing. We are now investigating if this can be remedied by further derivatization of the ligand framework with heavy atoms.

Experimental Section

Starting Materials and Analytical Procedures: Chemicals and solvents were purchased from Fluka A. G. and Aldrich. Solvents were purified by a non-hazardous procedure by passing them onto activated alumina columns (Innovative Technology Inc. System).[59] Stock solutions of lanthanides were prepared just before use in neat MeCN (previously dried on molecular sieves 4 Å) from the corresponding perchlorates $Ln(ClO_4)_3{\cdot}xH_2O$ (Ln = La, Nd, Eu, Gd, Er, Yb, x = 2.5–4.5). These salts were prepared from their oxides (99.99%, Rhodia Electronic and Catalysis or Research Chemicals, Phoenix Arizona) in the usual way.[60] Concentration of the solutions was determined by complexometric titrations using a standardized Na_2H_2EDTA solution in urotropine buffered medium and with xylenol orange as indicator.[61]

Analytical Measurements: NMR spectra were measured at 25 °C on Bruker Avance DRX 400 (^1H, 400 MHz), AV 600 (^{13}C, 150.864 MHz) and AV 800 (^{13}C, 201.54 MHz) spectrometers. Spectra of organic compounds were recorded in $CDCl_3$ (99.8%, Aldrich), CD_3OD (99.8%, Aldrich), [D_6]acetone (99.5%, Aldrich), [D_7]DMF (99.8%, Aldrich) and [D_6]DMSO (99.8%, Aldrich). Deuterated solvents were taken as internal standards; chemical shift values are given in ppm with respect to TMS and J values are reported in Hz. The ESI-MS spectra of the organic compounds were obtained on a Finningan TSQ 7100 spectrometer using 10^{-5} to 10^{-4} M solutions in acetonitrile/H_2O/formic acid (50:50:1) or MeOH; the capillary temperature was set to 180 °C and the ion spray voltage to 3.5 kV. The instrument was calibrated using horse myoglobin and the analyses were conducted in positive mode. ESI-TOF spectra in positive ion mode were recorded on a Q-TOF Ultima mass spectrometer (Micromass, Manchester, UK) equipped with a Z-spray type ESI source. Phosphoric acid was used for mass calibration in the range 500–2000 m/z. Data were acquired and processed with Masslynx version 4.0. Electrospray conditions were as follows: capillary voltage, 3 kV; source temperature, 80 °C; cone voltage, 35 V; source block temperature, 150 °C. The ESI nebulization and drying gas was nitrogen. The sample was introduced through a syringe pump operating at 20 μL min^{-1}. Simulation of spectra was achieved with Molecular Weight Calculator 6.42®. UV/Vis spectra and absorption spectrum of Yb^{III} ion were measured in 1.0 cm quartz Suprasil® cells on a Perkin–Elmer Lambda 900 spectrometer. Stability constants were determined by spectrophotometric titration of $(\mathbf{L^{ABX}})^-$ by Ln^{III} (Ln = La, Eu, Yb) in neat MeCN under N_2 atmosphere with the help of a J&M diode array spectrometer (Tidas series) connected to an external computer. All titrations were performed in a thermostatted (25.0 ± 0.1 °C) glass-jacketed vessel at μ = 0.1 M (KCl). Factor analysis[62] and mathematical treatment of the spectrophotometric data were performed with the Specfit® software.[63] Karl-Fischer titrations were performed by a Metrohm 836 Titrando potentiometer equipped with a Karl-Fischer 803 Ti block and a Pt electrode. Elemental analyses were performed by Dr. E. Solari, Elementary Analysis Laboratory of the Institute of Chemical Sciences and Engineering, EPFL.

Luminescence spectra and lifetimes were collected either on a Horiba-Jobin Yvon FL 3-22 fluorometer or on a home-made high-resolution set-up, according to procedures published previously.[64] Quantum yields were measured by a absolute method using a specially designed integration sphere.[56]

Synthesis of Ligands and Complexes

See Supporting Information for the synthesis of the intermediates.

6-(1,6-Dimethyl-11-oxo-6,11-dihydro-1*H*-imidazo[4,5-*a*]acridin-2-yl)-4-{2-[2-(2-methoxyethoxy)ethoxy]ethoxy}pyridine-2-carboxylic Acid (HL^{AB1}): An amount of $\mathbf{I_{19}}$ (90 mg, 0.157 mmol) was dissolved in absolute EtOH/H_2O (11.4 mL) solution containing NaOH (9.4 mg, 2.35×10^{-1} mmol). This mixture was stirred at room temperature for 16 h. After completion of the reaction, the solvents were removed under reduced pressure. The residue was dissolved in distilled water (25 mL) and the resulting aqueous solution was acidified to pH 2 by addition of hydrochloric acid 0.02 M. The acidic solution was then extracted with CH_2Cl_2 (5 × 100 mL), dried with Na_2SO_4 and the solvents evaporated. The crude product was triturated with hexane (100 mL), filtered and dried under vacuum to give a pale yellow solid (79 mg, 93% yield). ^1H NMR ([D_6]-DMSO) δ = 3.22 (s, 3 H, OCH_3), 3.42 (m, 2 H, H^6), 3.52 (m, 2 H, H^5), 3.55 (m, 2 H, H^4), 3.62 (m, 2 H, H^3), 3.83 (m, 2 H, H^2), 4.06 (s, 3 H, NCH_3), 4.30 (s, 3 H, NCH_3), 4.41 (m, 2 H, H^1), 7.39 (ddd, ^3J = 7.2, ^3J = 7.4, ^4J = 1.1 Hz, 1 H, H_{Ph}), 7.66 (d, ^4J = 2.4 Hz, 1 H, H_{Py}), 7.82 (ddd, ^3J = 6.8, ^3J = 7.4, ^4J = 1.2 Hz, 1 H, H_{Ph}), 7.85 (dd, ^3J = 7.2, ^4J = 1.2 Hz, 1 H, H_{Ph}), 7.92 (d, ^3J = 9.2 Hz, 1 H, $H_{Benz.}$), 7.92 (d, ^4J = 2.4 Hz, 1 H, H_{Py}), 8.19 (d, ^3J = 9.2 Hz, 1 H, $H_{Benz.}$), 8.37 (dd, ^3J = 6.8, ^4J = 1.1 Hz, 1 H, H_{Ph}) ppm. ^{13}C NMR (201.54 MHz, [D_6]DMSO): δ = 36.02 (NCH_3), 39.11 (NCH_3), 58.51 (OCH_3), 68.62 (OCH_2), 69.03 (OCH_2), 70.09 (OCH_2), 70.27 (OCH_2), 70.49 (OCH_2), 71.73 (OCH_2), 110.58 (CH_{Py}), 112.37 ($C_{Benz.\ quat.}$), 112.62 (CH_{Py}), 113.19 ($CH_{Benz.}$), 116.73 (CH_{Ph}), 121.94 (CH_{Ph}), 123.83 ($CH_{Benz.}$), 126.74 ($C_{Ph\ quat.}$), 126.93 (CH_{Ph}), 133.77 ($C_{Benz.Ph}$), 135.54 ($C_{Benz.\ quat.}$), 138.06 ($C_{Ph\ quat.}$), 141.85 (CH_{Ph}), 142.19 ($C_{Benz.\ quat.}$), 150.30 ($C_{Benz.\ quat.}$), 151.54 ($C_{Py\ quat.}$), 152.80 ($C_{Py\ quat.}$), 166.34 ($C_{Py\text{-}O\ quat.}$), 166.51 (*C*OOH), 175.66 (C=O) ppm. ESI-MS m/z calcd. for [M + H$^+$] (found): 547.22 (547.20). $C_{29}H_{30}N_4O_7{\cdot}0.25NaCl$ (561.19): calcd. C 62.11, H 5.39, N 9.99; found C 62.25, H 5.45, N 9.76.

6-(3,5-Dimethyl-10-oxo-5,10-dihydro-3*H*-imidazo[4,5-*b*]acridin-2-yl)-4-{2-[2-(2-methoxyethoxy)ethoxy]ethoxy}pyridine-2-carboxylic Acid (HL^{AB2}): An amount of $\mathbf{I_{29}}$ (290 mg, 0.504 mmol) was dissolved in EtOH/H_2O (35:13 mL) containing NaOH (30.3 mg, 0.758 mmol). This mixture was stirred at room temperature for 16 h. After completion of the reaction, the solvents were removed under reduced pressure. The residue was dissolved in distilled water (50 mL) and the resulting aqueous solution was acidified to pH 2 by addition of hydrochloric acid 0.02 M. The acidic solution was then extracted with $CHCl_3$ (5 × 250 mL), dried with Na_2SO_4 and the solvents evaporated. The crude product was triturated with hexane (150 mL), filtered and dried under vacuum to give a yellow-orange solid (262 mg, 95% yield). ^1H NMR ([D_6]DMSO): δ = 3.23 (s, 3 H, OCH_3), 3.42 (m, 2 H, H^6), 3.53 (m, 2 H, H^5), 3.56 (m, 2 H, H^4), 3.63 (m, 2 H, H^3), 3.84 (m, 2 H, H^2), 4.04 (s, 3 H, NCH_3),

4.43 (s, 3 H, NCH_3), 4.43 (m, 2 H, H^1), 7.29 (ddd, ^3J = 7.8, ^3J = 7.3, ^4J = 1.8 Hz, 1 H, H_{Ph}), 7.67 (d, ^4J = 2.5 Hz, 1 H, H_{Py}), 7.79 (dd, ^3J = 8.7, ^4J = 1.8 Hz, 1 H, H_{Ph}), 7.81 (dd, ^3J = 8.7, ^3J = 7.8 Hz, 1 H, H_{Ph}), 7.88 (s, 1 H, $H_{Benz.}$), 8.06 (d, ^4J = 2.5 Hz, 1 H, H_{Py}), 8.35 (d, ^3J = 7.3 Hz, 1 H, H_{Ph}), 8.66 (s, 1 H, $H_{Benz.}$) ppm. ^{13}C NMR (150.864 MHz, [D$_6$]DMSO): δ = 33.14 (NCH_3), 34.52 (NCH_3), 58.06 (OCH_3), 68.22 (OCH_2), 68.57 (OCH_2), 69.54 (OCH_2), 69.82 (OCH_2), 70.05 (OCH_2), 71.29 (OCH_2), 95.71 ($CH_{Benz.}$), 112.43 (CH_{Py}), 112.61 (CH_{Py}), 115.73 (CH_{Ph}), 117.06 ($C_{Benz.\ quat.}$), 119.25 (CH_{Ph}), 120.27 ($CH_{Benz.}$), 120.47 ($C_{Ph\ quat.}$), 126.68 ($C_{Benz.Ph}$), 133.92 (CH_{Ph}), 137.36 ($C_{Benz.\ quat.}$), 139.83 (CH_{Ph}), 142.26 ($C_{Ph\ quat.}$), 142.56 ($C_{Benz.\ quat.}$), 149.50 ($C_{Benz.\ quat.}$), 150.98 ($C_{Py\ quat.}$), 151.88 ($C_{Py\ quat.}$), 165.71 ($C_{Py\text{-}O\ quat.}$), 166.10 (*C*OOH), 177.11 (C=O) ppm. ESI-MS *m*/*z* calcd. for [M + H$^+$] (found): 547.22 (547.08), for [2M+H$^+$] (found): 1093.43 (1093.45). $C_{29}H_{30}N_4O_7$ (546.58): calcd. C 63.73, H 5.53, N 10.25; found C 63.25, H 5.53, N 10.13.

Synthesis of the Ln^{III} Complexes (General Procedure): The H**L^{ABX}** ligand was suspended in a ethanol/H_2O (5:5 mL) mixture followed by the addition of 1 mL of aqueous sodium hydroxide and subsequently stirred at room temperature for 15 min. to give a yellow solution. The solution was warmed up to 70–80 °C and $LnCl_3{\cdot}6H_2O$ in 1 mL of distilled water was added dropwise over 10 min. A yellow precipitate was formed and the resulting suspension was stirred for 30 min. After cooling, the precipitate was filtered, washed with distilled water (ca. 20 mL) and ethyl ether (ca. 20 mL). The precipitate so collected was then re-dissolved in CH_2Cl_2/MeOH (18:2 mL) or $CHCl_3$ (20 mL). The organic solution was concentrated under reduced pressure and subsequently dried under vacuum at room temperature to give colored solids.

[Eu(L^{AB1})$_3$]: The reaction was performed with H**L^{AB1}** (30 mg, 54.9 μmol), NaOH (2.56 mg, 0.641 mmol) and $EuCl_3{\cdot}6H_2O$ (6.71 mg, 0.183 mmol). Yellow-orange solid: 29.2 mg (88% yield). $C_{87}H_{87}EuN_{12}O_{21}{\cdot}2H_2O$ (1824.72): calcd. C 57.26, H 5.03, N 8.66; found C 57.22, H 5.19, N 9.21.

[Yb(L^{AB2})$_3$]: The reaction was performed with H**L^{AB2}** (40 mg, 0.732 mmol), NaOH (2.93 mg, 0.732 mmol) and $YbCl_3{\cdot}6H_2O$ (9.46 mg, 0.244 mmol). Brown-orange solid: 43.3 mg (98% yield). $C_{87}H_{87}N_{12}O_{21}Yb{\cdot}H_2O$ (1827.77): calcd. C 57.17, H 4.91, N 9.20; found C 57.43, H 5.20, N 9.29.

Supporting Information (see also the footnote on the first page of this article): Syntheses of all intermediates; data of ESI-TOF mass spectra for lanthanide complexes (Tables S1, S2); absorption spectra, distribution diagrams and recalculated absorption spectra for spectrophotometric titrations of ligands (**L^{ABX}**)$^-$ by lanthanide perchlorates (Figures S1–S9); absorption spectra of ligand (**L^{AB2}**)$^-$ and its complexes (Figure S10) and luminescence spectra of ligands (**L^{ABX}**)$^-$ and some of their complexes in neat MeCN at both 77 (with a 50 μs time delay) and 295 K (Figures S11, S12)

Acknowledgments

This research is supported by the Swiss National Science Foundation (grant 200020_119866). J. C. B. thanks the World Class University (WCU) program of the National Science Foundation of Korea (Ministry of Education, Science, and Technology) for a grant (R31-10035).

[1] S. Comby, J.-C. G. Bünzli, *Lanthanide Near-Infrared Luminescence in Molecular Probes and Devices*, Handbook on the Physics and Chemistry of Rare Earths (Eds.: K. A. Gschneidner Jr., J.-C. G. Bünzli, V. K. Pecharsky), Elsevier Science B. V., Amsterdam, **2007**, vol. 37, chapter 235, p. 217–470.
[2] J.-C. G. Bünzli, A.-S. Chauvin, C. D. B. Vandevyver, B. Song, S. Comby, *Ann. N. Y. Acad. Sci.* **2008**, *1130*, 97–105.
[3] S. V. Eliseeva, J.-C. G. Bünzli, *Chem. Soc. Rev.* **2010**, *39*, 189–227.
[4] P. He, H. H. Wang, S. G. Liu, J. X. Shi, G. Wang, M. L. Gong, *Inorg. Chem.* **2009**, *48*, 11382–11387.
[5] S. Pandya, J. H. Yu, D. Parker, *Dalton Trans.* **2006**, 2757–2766.
[6] A. D'Aléo, A. Picot, P. L. Baldeck, C. Andraud, O. Maury, *Inorg. Chem.* **2008**, *47*, 10269–10279.
[7] A. D'Aléo, G. Pompidor, B. Elena, J. Vicat, P. L. Baldeck, L. Toupet, R. Kahn, C. Andraud, O. Maury, *ChemPhysChem* **2007**, *8*, 2125–2132.
[8] L. M. Fu, X. F. Wen, X. C. Ai, Y. Sun, Y. S. Wu, J. P. Zhang, Y. Wang, *Angew. Chem. Int. Ed.* **2005**, *44*, 747–750.
[9] M. H. V. Werts, N. Nerambourg, D. Pelegry, Y. Le Grand, M. Blanchard-Desce, *Photochem. Photobiol. Sci.* **2005**, *4*, 531–538.
[10] G. Piszczek, B. P. Maliwal, I. Gryczynski, J. Dattelbaum, J. R. Lakowicz, *J. Fluoresc.* **2001**, *11*, 101–107.
[11] M. J. Levene, D. A. Dombeck, K. A. Kasischke, R. P. Molloy, W. W. Webb, *J. Neurophysiology* **2004**, *91*, 1908–1912.
[12] S. Faulkner, L. S. Natrajan, W. S. Perry, D. Sykes, *Dalton Trans.* **2009**, 3890–3899.
[13] H. B. Xu, L. Y. Zhang, Z. H. Chen, L. X. Shi, Z. N. Chen, *Dalton Trans.* **2008**, *18*, 4664–4670.
[14] F. F. Chen, Z. Q. Bian, Z. W. Liu, D. B. Nie, Z. Q. Chen, C. H. Huang, *Inorg. Chem.* **2008**, *47*, 2507–2513.
[15] M. D. Ward, *Coord. Chem. Rev.* **2007**, *251*, 1663–1677.
[16] R. Ziessel, S. Diring, P. Kadjane, L. J. Charbonnière, P. Retailleau, C. Philouze, *Chem. Asian J.* **2007**, *2*, 975–982.
[17] J.-C. G. Bünzli, C. Piguet, *Chem. Soc. Rev.* **2005**, *34*, 1048–1077.
[18] G. A. Hebbink, L. Grave, L. A. Woldering, D. N. Reinhoudt, F. C. J. M. Van Veggel, *J. Phys. Chem. A* **2003**, *107*, 2483–2491.
[19] W. Huang, D. Wu, D. Guo, X. Zhu, C. He, Q. Meng, C. Duan, *Dalton Trans.* **2009**, 2081–2084.
[20] M. Albrecht, O. Osetska, J.-C. G. Bünzli, F. Gumy, R. Fröhlich, *Chem. Eur. J.* **2009**, *15*, 8791–8799.
[21] A. Nonat, D. Imbert, J. Pécaut, M. Giraud, M. Mazzanti, *Inorg. Chem.* **2009**, *48*, 4207–4218.
[22] S. Comby, D. Imbert, C. D. B. Vandevyver, J.-C. G. Bünzli, *Chem. Eur. J.* **2007**, *13*, 936–944.
[23] N. M. Shavaleev, S. J. A. Pope, Z. R. Bell, S. Faulkner, M. D. Ward, *Dalton Trans.* **2003**, 808–814.
[24] R. Ziessel, G. Ulrich, L. J. Charbonnière, D. Imbert, R. Scopelliti, J.-C. G. Bünzli, *Chem. Eur. J.* **2006**, *12*, 5060–5067.
[25] C. Yang, L. M. Fu, Y. Wang, J. P. Zhang, W. T. Wong, X. C. Ai, Y. F. Qiao, B. S. Zou, L. L. Gui, *Angew. Chem. Int. Ed.* **2004**, *43*, 5010–5013.
[26] Y. Bretonniere, M. J. Cann, D. Parker, R. Slater, *Org. Biomol. Chem.* **2004**, *2*, 1624–1632.
[27] A. Dadabhoy, S. Faulkner, P. G. Sammes, *J. Chem. Soc. Perkin Trans. 2* **2002**, 348–357.
[28] M. H. V. Werts, M. A. Duin, J. W. Hofstraat, J. W. Verhoeven, *Chem. Commun.* **1999**, 799–800.
[29] R. Van Deun, P. Nockemann, P. Fias, K. Van Hecke, L. Van Meervelt, K. Binnemans, *Chem. Commun.* **2005**, 590–592.
[30] T. Faller, K. Hutton, G. Okafo, A. Gribble, P. Camilleri, D. E. Games, *Chem. Commun.* **1997**, 1529–1530.
[31] J. L. Reymond, T. Koch, J. Schroer, E. Tierney, *Proc. Natl. Acad. Sci. USA* **1996**, *93*, 4251–4256.
[32] N. M. Shavaleev, R. Scopelliti, F. Gumy, J.-C. G. Bünzli, *Inorg. Chem.* **2009**, *48*, 5611–5613.
[33] E. M. Davis, T. N. Nanninga, H. I. Tjiong, D. D. Winkle, *Org. Process Res. Dev.* **2005**, *9*, 843–846.
[34] A. Boumendjel, S. Macalou, A. Ahmed-Belkacem, M. Blanc, A. Di Pietro, *Bioorg. Med. Chem.* **2007**, *15*, 2892–2897.
[35] Z. Daszkiewicz, J. B. Kyziol, *J. Prakt. Chem.* **1988**, *330*, 44–50.

[36] D. Suzuki, R. Kiluchi, M. Yasui, **2002**, *US Patent*, U. S. 6403789 B1.
[37] A.-S. Chauvin, S. Comby, B. Song, C. D. B. Vandevyver, J.-C. G. Bünzli, *Chem. Eur. J.* **2008**, *14*, 1726–1739.
[38] E. Deiters, B. Song, A.-S. Chauvin, C. Vandevyver, J.-C. G. Bünzli, *Chem. Eur. J.* **2009**, *15*, 885–900.
[39] M. A. Phillips, *J. Chem. Soc.* **1928**, 172–177.
[40] C. Piguet, J.-C. G. Bünzli, *Self-assembled Lanthanide Helicates: from Basic Thermodynamics to Applications*, Handbook on the Physics and Chemistry of Rare Earths (Eds.: K. A. Gschneidner Jr., J.-C. G. Bünzli, V. K. Pecharsky), Elsevier Science B. V., Amsterdam, **2010**, vol. 40, ch, 247, pp. 351–553.
[41] M. Elhabiri, R. Scopelliti, J.-C. G. Bünzli, C. Piguet, *J. Am. Chem. Soc.* **1999**, *121*, 10747–10762.
[42] S. Petoud, J.-C. G. Bünzli, F. Renaud, C. Piguet, K. J. Schenk, G. Hopfgartner, *Inorg. Chem.* **1997**, *36*, 5750–5760.
[43] E. Deiters, B. Song, A.-S. Chauvin, C. D. B. Vandevyver, J.-C. G. Bünzli, *New J. Chem.* **2008**, *32*, 1140–1152.
[44] T. Le Borgne, P. Altmann, N. André, J.-C. G. Bünzli, G. Bernardinelli, P.-Y. Morgantini, J. Weber, C. Piguet, *Dalton Trans.* **2004**, 723–733.
[45] S. Tobita, M. Arakawa, I. Tanaka, *J. Phys. Chem.* **1985**, *89*, 5649–5654.
[46] J.-C. G. Bünzli, B. Klein, D. Wessner, N. W. Alcock, *Inorg. Chim. Acta* **1982**, *59*, 269–274.
[47] S. T. Frey, W. d. Horrocks Jr., *Inorg. Chim. Acta* **1995**, *229*, 383–390.
[48] C. Piguet, J.-C. G. Bünzli, G. Bernardinelli, G. Hopfgartner, S. Petoud, O. Schaad, *J. Am. Chem. Soc.* **1996**, *118*, 6681–6697.
[49] S. Petoud, J.-C. G. Bünzli, T. Glanzman, C. Piguet, Q. Xiang, R. P. Thummel, *J. Lumin.* **1999**, *82*, 69–79.
[50] F. R. Gonçalves e Silva, R. L. Longo, O. L. Malta, C. Piguet, J.-C. G. Bünzli, *Phys. Chem. Chem. Phys.* **2000**, *2*, 5400–5403.
[51] R. Van Deun, P. Nockemann, T. N. Parac-Vogt, K. Van Hecke, L. Van Meervelt, C. Görller-Walrand, K. Binnemans, *Polyhedron* **2007**, *26*, 5441–5447.
[52] F. L. Jiang, W. K. Wong, X. J. Zhu, G. J. Zhou, W. Y. Wong, P. L. Wu, H. L. Tam, K. W. Cheah, C. Ye, Y. Liu, *Eur. J. Inorg. Chem.* **2007**, 3365–3374.
[53] A. D'Aléo, A. Picot, A. Beeby, J. A. Gareth Williams, B. Le Guennic, C. Andraud, O. Maury, *Inorg. Chem.* **2008**, *47*, 10258–10268.
[54] J. Zhang, S. Petoud, *Chem. Eur. J.* **2008**, *14*, 1264–1272.
[55] N. M. Shavaleev, R. Scopelliti, F. Gumy, J.-C. G. Bünzli, *Inorg. Chem.* **2009**, *48*, 7937–7946.
[56] A. Aebischer, F. Gumy, J.-C. G. Bünzli, *Phys. Chem. Chem. Phys.* **2009**, *11*, 1346–1353.
[57] M. H. V. Werts, R. T. F. Jukes, J. W. Verhoeven, *Phys. Chem. Chem. Phys.* **2002**, *4*, 1542–1548.
[58] A. Beeby, I. M. Clarkson, R. S. Dickins, S. Faulkner, D. Parker, L. Royle, A. S. de Sousa, J. A. G. Williams, M. Woods, *J. Chem. Soc. Perkin Trans. 2* **1999**, 493–503.
[59] A. B. Pangborn, M. A. Giardello, R. H. Grubbs, R. K. Rosen, F. J. Timmers, *Organometallics* **1996**, *15*, 1518–1520.
[60] J.-C. G. Bünzli, C. Mabillard, *Inorg. Chem.* **1986**, *25*, 2750–2754.
[61] G. Schwarzenbach, *Complexometric Titrations*, Chapman & Hall, London, **1957**.
[62] E. R. Malinowski, D. G. Howery, *Factor Analysis in Chemistry*, John Wiley, New York, Chichester, Brisbane, Toronto, **1991**.
[63] H. Gampp, M. Maeder, C. J. Meyer, A. D. Zuberbühler, *Talanta* **1986**, *33*, 943–951.
[64] R. Rodriguez-Cortinas, F. Avecilla, C. Platas-Iglesias, D. Imbert, J.-C. G. Bünzli, A. de Blas, T. Rodriguez-Blas, *Inorg. Chem.* **2002**, *41*, 5336–5349.

Received: November 26, 2009
Published Online: February 11, 2010

